Available online at www.sciencedirect.com
ScienceDirect
Trans. Nonferrous Met. Soc. China 20(2010) 1615−1621
Transactions of Nonferrous Metals Society of China
www.tnmsc.cn

Microstructural evolution during partial remelting of AM60B magnesium alloy refined by $MgCO_3$

CHEN Ti-jun(陈体军), MA Ying(马 颖), WANG Rui-quan(王瑞全), LI Yuan-dong(李元东), HAO Yuan(郝 远)

Key Laboratory of Gansu Advanced Nonferrous Metal Materials,
Lanzhou University of Technology, Lanzhou730050, China

Received 13 May 2010; accepted 20 June 2010

Abstract: AM60B magnesium alloy was refined by $MgCO_3$ and its microstructural evolution was investigated during partial remelting. The results indicate that $MgCO_3$ is an effective grain refiner for AM60B alloy and can decrease the grain size from 329 μm of the unrefined alloy to 69 μm. A semisolid microstructure with small and spheroidal primary particles can be obtained after being partially remelted. The microstructure evolution can be divided into four steps: the initial rapid coarsening, structure separation, spheroidization and final coarsening. Correspondingly, these four steps result from the phase transformations of $\beta\rightarrow\alpha$, $\alpha+\beta\rightarrow L$ and $\alpha\rightarrow L$, $\alpha\rightarrow L$ and two reverse reactions of $\alpha\rightarrow L$ and $L\rightarrow\alpha$, respectively. One spheroidal primary particle in the semisolid microstructure usually originates one dendrite in the as-cast microstructure. The variation of primary particle size with holding time does not obey the LSW law, $D_t^3-D_0^3=Kt$, after the semisolid system is in its solid-liquid equilibrium state. Longer heating duration makes the primary particles more globular, but it makes their size larger at the same time.
Key words: AM60B alloy; thixoforming; microstructure evolution; phase transformation; partial remelting

1 Introduction

Thixoforming is one kind of semisolid metal processing. It is no longer a novel, but rather a powerful technology for forming alloys in semi-solid state to near net shaped components. Millions of aluminium alloy products are produced using this technology every year in Europe, Japan and USA[1]. But for magnesium alloys, the investigations on thixoforming are obviously laggard to those of aluminum alloys. So far, only one technique, thixomoulding, has been employed in practice[2]. Therefore, it is necessary to pay more attention to magnesium alloys.

It is well known that the key procedure of thixoforming is to produce semisolid microstructure with small and spheroidal primary particles uniformly suspended in liquid phase. There are several methods to fabricate this kind of nondendritic semisolid microstructure. Among them, grain refining process produces the desired microstructure by adding grain refiner during traditional casting and a following heat treatment in mushy zone. It is a relatively simple method because it does not need special treating procedures, such as stirring, spraying or deformation[3−4]. The key of this method is to obtain cast ingots with fine equiaxed grains. However, for AM60B alloy, a most commonly used aluminum-bearing magnesium alloy, there is still no commercial refiner although some investigations indicate that carbon inoculation is an effective grain refining technique[5]. In addition, the microstructural evolution during partial remelting is another key topic because this process has large effect on the resultant semisolid microstructure. Unfortunately, most of the existing investigations have been focused on the previously deformed Mg alloys [3−4, 6−8]. Only a few works have involved the as-cast alloys and emphasized on the morphology change and coarsening behavior of the primary particles or the Mg_2Si particles in Si-containing alloys in semisolid state[9−11]. However, the microstructural evolution prior to liquid formation is very important for the final semisolid microstructure[12]. Furthermore, the relations between the as-cast microstructure and semisolid microstructure are still unclear. Finally, it can be expected that the microstructural evolution essentially results from the phase transformations occurring during partial remelting and study on the phase transformations can

Foundation item: Project(G2007CB613706) supported by the National Basic Research Program of China
Corresponding author: CHEN Ti-jun; Tel: +86-931-29766573; E-mail: chentj@lut.cn, chentj1971@126.com
DOI: 10.1016/S1003-6326(09)60348-4

offer some important information to further verify the microstructural evolution.

Therefore, in this work, AM60B alloy is grain-refined by $MgCO_3$ and its microstructural evolution is investigated during partial remelting. Simultaneously, the phase transformations occurring during partial remelting are also discussed.

2 Experimental

The alloy used in this work is commercial AM60B magnesium alloy and its composition is Mg-5.98Al-0.343Mn-0.023Si (mass fraction, %). A quantity of the alloy was first remelted at 740 °C and degassed by C_2Cl_6. The melt then was heated to 790 °C and 1.2% (mass fraction) $MgCO_3$ was added. After being held for 10 min, the melt was cooled to 720 °C and poured into a permanent mould at ambient temperature to form some rods (*d*16 mm×150 mm). The rods were cut into small specimens (*d*16 mm×10 mm). The specimens were heated for different durations (0−90 min) at semisolid temperature of 610 °C and then water-quenched quickly. The temperature in the specimen was examined by a thermocouple that was mounted in the center of the specimen.

One cross-section of each specimen was processed by standard metallographic techniques, and then examined by energy disperse spectroscopy (EDS). Subsequently, they were etched by 4% (volume fraction) HNO_3 aqueous solution and observed on an optical microscope. The size and shape factor of primary particles in the semisolid microstructures were quantitatively examined. The details about the examinations can be found in Ref.[12]. On each sample, three images were examined. X-ray diffractometer (XRD) was used to identify the phase constituents in order to deduce the phase transformations occurring during partial remelting.

3 Results and discussion

3.1 Grain refinement of AM60B alloy by $MgCO_3$

Figs.1(a) and (b) show the as-cast microstructures of the unrefined alloy and the refined alloy by 1.2% $MgCO_3$, respectively. It can be seen that the primary grains of the unrefined alloy are very developed dendrites and their secondary dendrite arms are more than 100 μm long (Fig.1(a)). After being treated by $MgCO_3$, the primary grains have been significantly refined and they become into small and uniform equiaxed dendrites (Fig.1(b)). This change in grain size can be more clearly seen by comparing the microstructures as shown in Figs.1(c) and (d) of these two alloys after being solution treated. The quantitative examination shows that the grain size of the unrefined alloy is up to 329 μm while that of the refined alloy is

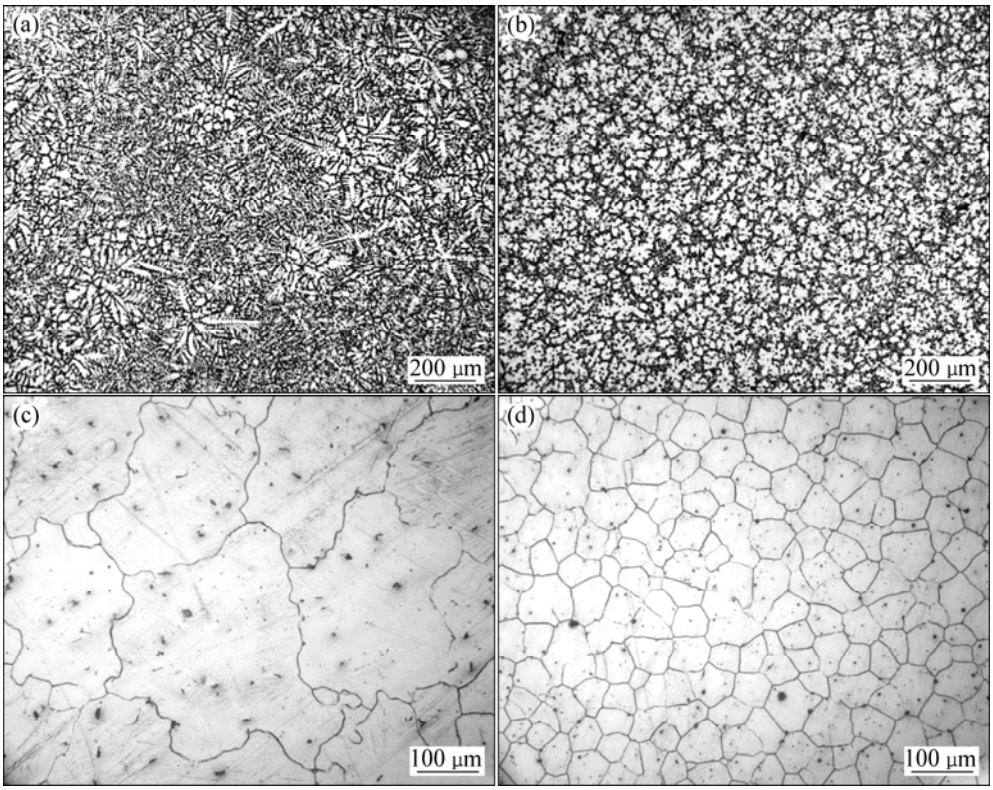

Fig.1 As-cast microstructures of unrefined (a) and refined (b) AM60B alloys, and solution-treated microstructures of unrefined (c) and refined (d) AM60B alloys

only 69 μm. This implies that $MgCO_3$ is an effect grain refiner for AM60B magnesium alloy and the treating technique employed in this work is appropriate.

For the carbon inoculation of Al-bearing magnesium alloys, the heterogeneous nucleation mechanism taking Al_4C_3 particles as nuclei has been commonly accepted although there is no direct evidence[5, 13−14]. When the reagent of $MgCO_3$ is added into the melt, it will decompose according to the following reaction:

$$MgCO_3 \longrightarrow MgO+CO_2 \quad (1)$$

The formed CO_2 then reacts with Mg:

$$2Mg+CO_2 \longrightarrow 2MgO+C \quad (2)$$

Finally, the reduced C reacts with Al to form Al_4C_3:

$$3C+4Al \longrightarrow Al_4C_3 \quad (3)$$

Both the formed Al_4C_3 and α-Mg are of close-packed hexagonal lattice and the smallest planar disregistry between them is 3.35%, much less than 15%, the critical value for the nucleation particles to act as heterogeneous nuclei[13−14]. Therefore, the Al_4C_3 particles can act as the efficient heterogeneous nuclei for AM60B magnesium alloy and the addition of $MgCO_3$ can significantly refine its grains.

3.2 Microstructural evolution during partial remelting

Fig.2 shows the microstructures of the refined AM60B alloys heated for different durations at semisolid temperature of 610 °C. It is indicated that the equiaxed dendrite morphology in the as-cast microstructure is relatively obvious. The dendrite is surrounded by discontinuous eutectic β phase ($Mg_{17}Al_{12}$) and the neighboring dendrite arms are separated each other by eutectic α phase (Fig.2(a)). The eutectic β phase between the dendrite arms is in small dot-like particle form. Through comparing Figs.2(a)−(c), three phenomena can be found during heating from 0 min to 3 min: 1) the amount of β phase decreases as the heating time increases; 2) the contrast difference between the eutectic α phase and the primary α phase becomes undistinguishable, resulting in the gradual disappearance of the dendrite morphology; 3) the residual eutectic β phase melts to form the liquid phase after being heated for 3 min. According to Mg-Al binary phase diagram, AM60B alloy will experience a single α phase interval during heating[15]. So, the β phase dissolves towards the primary α phase, resulting in the decrease of its amount. However, the temperature rise of the specimen is very rapid during this period as shown by Fig.3 and there is not enough time for β phases to completely dissolve, so some of them is left when the temperature reaches eutectic reaction point. The residual β phases then melt to form the liquid phase. In addition, because of the composition homogenization resulting from the temperature rise, the difference between the primary α phase and the eutectic α phase decreases. Simultaneously, most of the β phases between the dendrite arms dissolve, even disappear. So, it can be expected that due to the homogenization and dissolution, the boundaries between

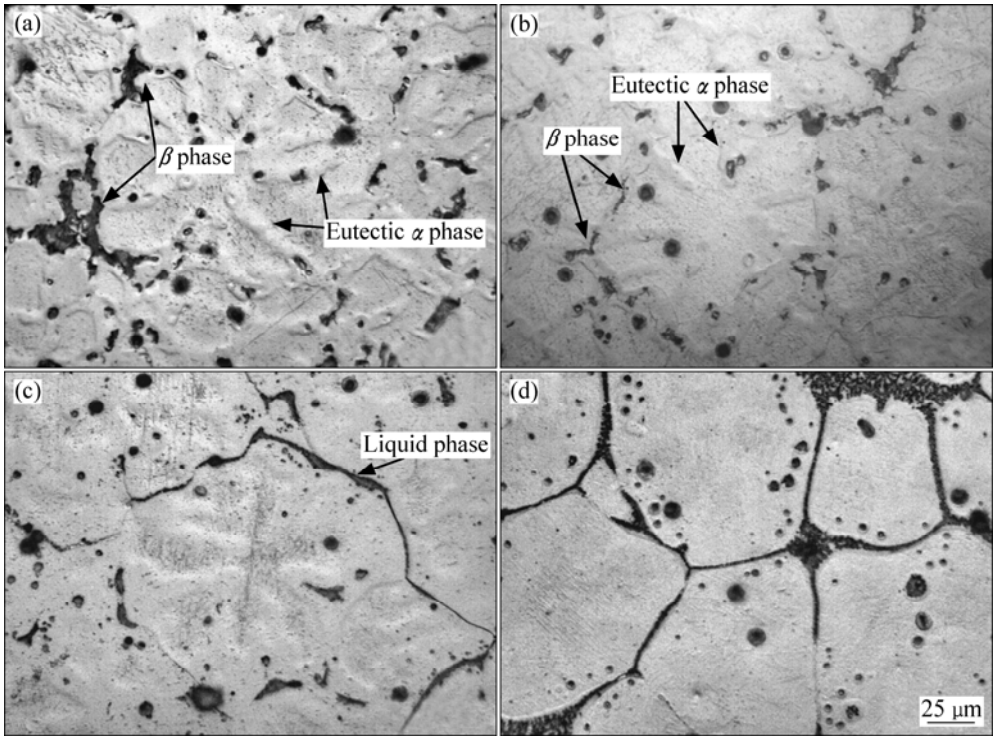

Fig.2 Microstructures of refined AM60B alloys heated at 610 °C for different times: (a) 0 min; (b) 2 min; (c) 3 min; (d) 10 min

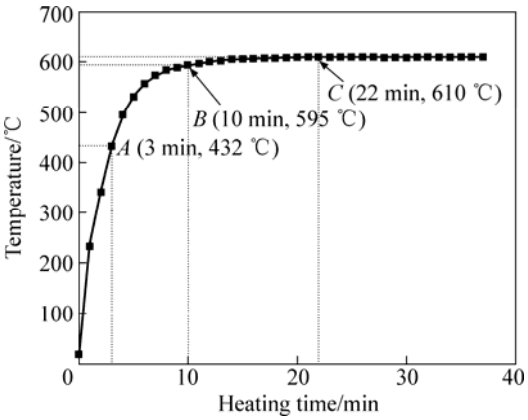

Fig.3 Temperature variation in specimen with heating time

the dendrite arms become undistinguishable and the original dendrite morphology becomes indistinct.

Furthermore, these two behaviors lead the neighboring dendrite arms to grow together or merge, and thus lead the morphology of the primary phase to change from the original equiaxed dendrite shape to the near-spheroidal particle form. Therefore, it can be concluded that, in view of the microstructural evolution, the coarsening of the dendrites resulting from the dissolution of eutectic is the main event during the period from 0 min to 2 min.

As described above, the residual β phase has melted to form liquid phase when being heated for 3 min. But it can be seen that the amount of the liquid phase in Fig.2(c) is larger than that of the residual β phases in Fig.2(b), which implies that the residual β phases have melted before heating for 3 min and some extra liquid phase has also formed when being heated for 3 min. It can be expected that the composition homogenization can also lead the neighboring dendrites to grow together at some local sites where the eutectic, especially eutectic β phase, has completely dissolved. But the energy at these contact sites (i.e. the part of the original grain boundaries) is higher than that within the dendrite due to crystal misorientation. So, the first formed liquid phase from the melting of residual eutectic penetrates along these sites or these sites directly melt during the subsequent heating (Fig.2(c)), which leads the coarsened dendrites (near spheroidal particles) to separate from their neighboring dendrites to form individual polygonal particles (Fig.2(d)). Figs.2(d) and Fig.4(a) show that the original dendrites have evolved into the individual polygonal particles which are separated by thin liquid layers after being heated for 10 min. So, it can be suggested that the structure separation is the second step of the microstructural evolution and this step results from the melting of residual eutectic and penetration of the first formed liquid along the original grain boundaries.

As the heating further proceeds, the polygonal particles partially melt due to the continuous rise of the

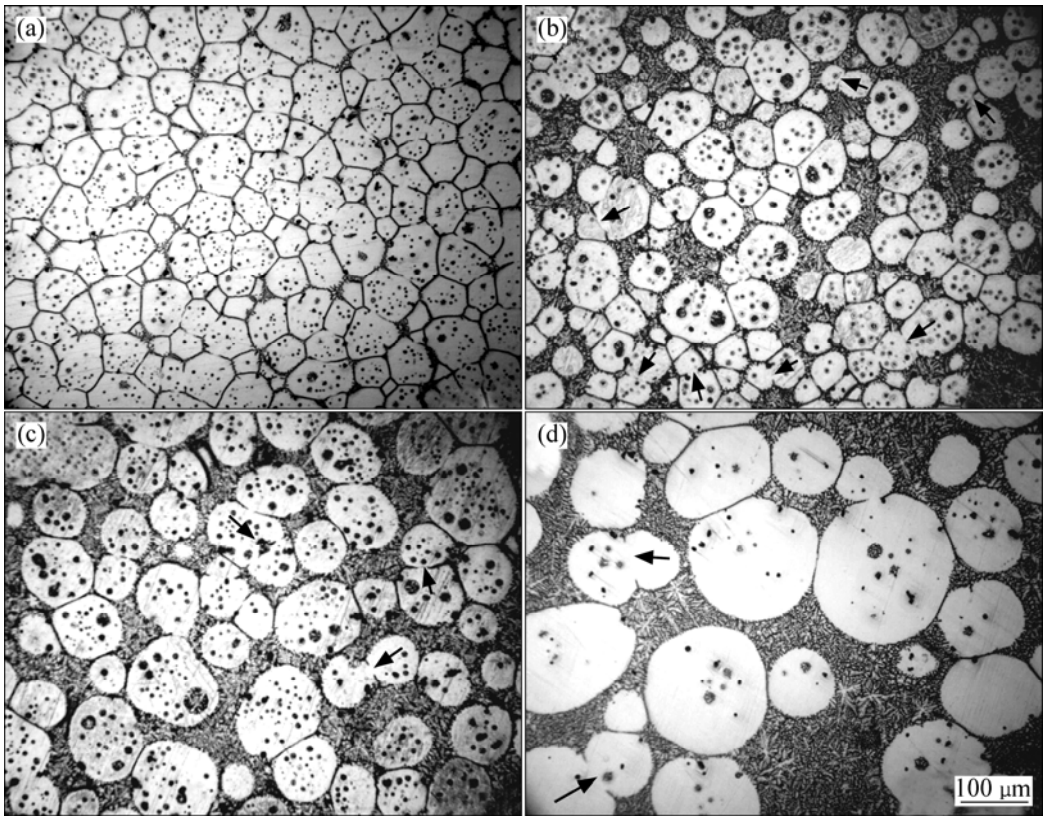

Fig.4 Microstructures of refined AM60B alloys heated at 610 °C for different time: (a) 10 min; (b) 20 min; (c) 30 min; (d) 90 min

temperature (Fig.3). It is well known that the surface curvature of a crystal has great effect on its melting point: the larger the curvature, the lower the melting point[16]. So, the edges and corners of the polygonal particle preferentially melt, which not only increases the liquid phase amount, but also leads the particles to become spheroidal (Figs.4(a)−(c)). Fig.4(b) shows that a semisolid microstructure with small and spheroidal particles and suitable liquid fraction (about 50%, volume fraction) is obtained when the specimen is heated for 20 min. Fig.3 indicates that the specimen temperature is up to the final value of 610 °C after being heated for 22 min. It can be suggested that this partial melting continues till the temperature reaches 610 °C. Based on the above discussion, it can be concluded that the spheroidization of the polygonal particles is the main event occurring during period from 10 min to 22 min. In addition, one spheroidal particle in the semisolid microstructure originates one equiaxed dendrite in the as-cast microstructure.

After being heated for 22 min, it can be found that the primary particles gradually become large and more spheroidal with the increase of heating time (Figs.4(c) and (d)). In addition, the liquid fraction does not change and maintains a constant of 51%. This indicates that the semisolid system is up to its solid-liquid equilibrium state at this time. Fig.5 presents the variations of the particle size and shape factor with the heating time in 10−90 min. If the variation of particle size with the holding time obeys the formula, $D_t^3 - D_0^3 = Kt$ (where D_t is the average particle size at time t, D_0 is the initial particle size and K is the coarsening rate constant), after a semisolid system reaches its equilibrium sate, the coarsening should result from Ostwald ripening[17]. But the present result (taking heating for 30 min as the start time, t=0) does not obey this regime as shown in Fig.6. It can be found that there are always some agglomerates

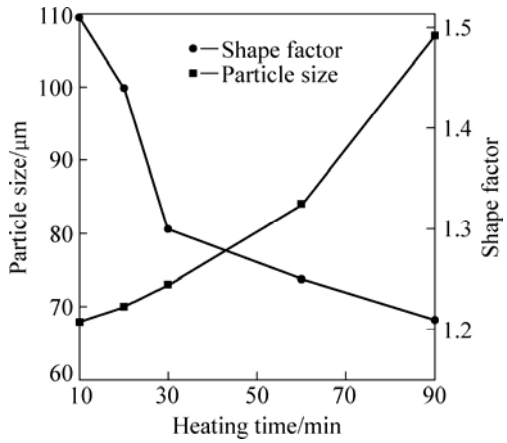

Fig.5 Variations of particle size and shape factor with heating time

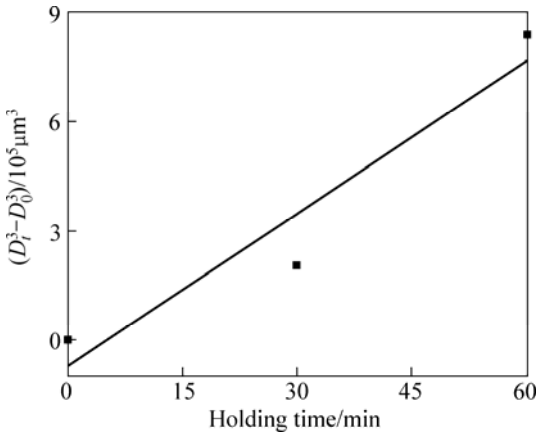

Fig.6 Cube of primary particle size versus holding time, taking 30 min as starting time (t=0)

composed of two bonded particles (marked by arrows in Figs.3(b) and (c)), which implies that the coarsening from mergence plays an important role even after the system is up to the equilibrium state. However, it should be noted that Ostwald ripening also operates at the same time. Because Ostwald ripening also includes the dissolution of edges and corners of the particles and the subsequent reprecipitation at sunken zones[17−18], the particles become more and more spheroidal and the shape factor decreases (Figs.3(c), (d) and Fig.5). On the whole, the coarsening of the primary particles is the final steps of the microstructural evolution.

Based on the above discussion, it can be concluded that the microstructural evolution includes four steps: the initial coarsening due to the dissolution of eutectic towards the primary dendrites, the structure separation resulted from the melting of residual eutectic and subsequent penetration of the first formed liquid phase along the original grain boundaries, the spheroidization attributed to the melting of edges and corners of the polygonal particles, and the final coarsening owing to the mergence and Ostwald ripening.

3.3 Phase transformations and their relations with microstructural evolution

As discussed above, the main event occurring during heating from 0 min to about 3 min is the coarsening of dendrites through mergence of dendrite arms. The essential of this behavior is the dissolution of eutectic β phase towards the primary α phase. From the aspect of phase transformation, this behavior can be expressed as the reaction of $\beta \rightarrow \alpha$. Due to this reaction, the amount of β phase decreases (comparing Fig.2(a) with (b)). This result can also be found by comparing the corresponding diffraction intensities shown in Fig.7. It is also due to this reaction (i.e., the dissolution of the

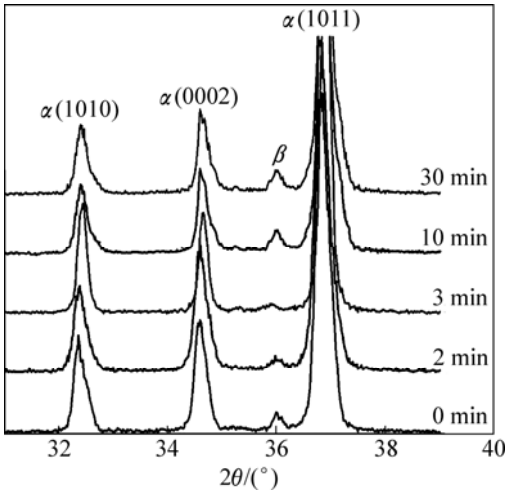

Fig.7 XRD patterns of AM60B alloys heated at 610 °C for different times and then water-quenched

Table 1 Chemical compositions of different structures of AM60B alloys heated for different durations at 610 °C and then water-quenched (mass fraction, %)

Heating time/min	Structure	Mg	Al	Mn
0	Primary α	93.90	6.10	0
	Eutectic β	78.99	21.01	0
2	Primary α	91.46	8.57	0
	Eutectics β	83.46	16.54	0
3	Primary α	89.70	10.3	0
	Liquid phase	87.77	12.23	0
10	Primary α	85.24	14.14	0.62
	Liquid phase	91.61	8.39	0
30	Primary α	88.46	10.78	0.76
	Liquid phase	93.39	6.61	0

Al-rich β phase) that the Al content of primary α phase increases (Table 1).

When the temperature of the specimen reaches the eutectic reaction point, the residual eutectic β phase melts to form liquid phase. This can be expressed by the reverse eutectic reaction of $\alpha+\beta\rightarrow L$. According to the discussion in above section, this reaction should complete in a short period before 3 min (i.e. a short period before point A in Fig.3). Because some Mg-rich α phase surrounding the eutectic β phase also melts through this reaction, the Al content in the liquid phase decreases compared with that of the β phase (Table 1). As the heating is further prolonged, the first formed liquid phase penetrates along the original grain boundaries or the grain boundaries directly melt to separate the near spheroidal particles (coarsened dendrites) from their neighboring particles due to the temperature rise. Then, the microstructure evolves into the individual polygonal particles separated by thin liquid layers. According to the Mg-Al binary phase diagram or the solidification process of AM60B alloy[15], this penetration or melting essentially results from the reaction of $\alpha\rightarrow L$. Also owing to the melting of some Mg-rich α phase, the Al content in the liquid phase further decreases (Table 1). After being water-quenched, the liquid phase again solidifies into the primary α phase and $\alpha+\beta$ eutectic structures. So, the diffraction intensity of the β phase again increases during the period of 3−10 min (Fig.7). Therefore, it can be concluded that the structure separation should be attributed to the reactions of $\alpha+\beta\rightarrow L$ and $\alpha\rightarrow L$.

After being heated for 10 min, the temperature of the specimen is up to 595 °C as shown by point B in Fig.3, and the alloy is in the $L+\alpha$ two-phase interval. During the period from 10 min to 22 min, the spheroidization occurs through the melting of edges and corners of the primary α phase polygonal particles. In view of phase transformation, this process can be presented as the reaction of $\alpha\rightarrow L$. Due to the melting of large amount of α phase through this reaction, the Al content in the liquid phase obviously decreases (Table 1). In addition, the solubility of Al in the α phase decreases as the temperature rises. So, the extra Al element diffuses into the liquid phase and its content in the α phase particles decreases during this period (Table 1). Furthermore, there is no extra liquid phase which can form β phase after being water-quenched, so the diffraction intensity of β phase almost does not change after 10 min (Fig.7).

After the semisolid system reaches its final solid-liquid equilibrium state, the main event is the coarsening of the primary particles due to the mergence and Ostwald ripening. The mergence is operated through grain boundary migration or grain rotation (that minimizes misorientation)[19], which does not involve phase transformation. But Ostwald ripening essentially refers to the dissolution and subsequent reprecipitation[17−18]. From the aspect of phase transformation, these two reverse processes can be expressed by the two reverse reactions of $\alpha\rightarrow L$ and $L\rightarrow\alpha$ respectively. That is to say, the final coarsening partially results from the reactions of $\alpha\rightarrow L$ and $L\rightarrow\alpha$.

Summarizing the above discussion, the phase transformations occurring during partial remelting and their relations with the microstructural evolution can be schematically presented by Fig.8. This indicates that the initial coarsening is due to the reaction of $\beta\rightarrow\alpha$, the structure separation results from $\alpha+\beta\rightarrow L$ and $\alpha\rightarrow L$, the spheroidization is attributed to $\alpha\rightarrow L$ and the final coarsening is partially ascribed to the two reverse reactions of $\alpha\rightarrow L$ and $L\rightarrow\alpha$.

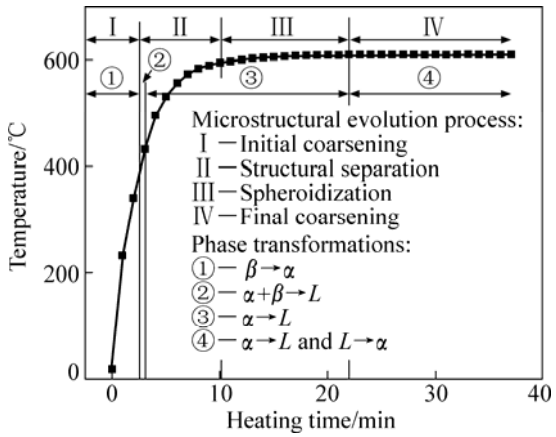

Fig.8 Schematic diagram of microstructural evolution and phase transformations during partial remelting

4 Conclusions

1) $MgCO_3$ is an effective grain refiner for AM60B alloy and can decrease the grain size from 329 μm of the unrefined alloy to 69 μm.

2) A semisolid microstructure with small and spheroidal primary particles can be obtained after the grain-refined AM60B alloy is partially remelted.

3) The microstructure evolution during partial remelting includes four steps: the initial rapid coarsening, structure separation, spheroidization and final coarsening. Correspondingly, these four steps completely or partially result from the phase transformations of $\beta\rightarrow\alpha$, $\alpha+\beta\rightarrow L$ and $\alpha\rightarrow L$, $\alpha\rightarrow L$ and two reverse reactions of $\alpha\rightarrow L$ and $L\rightarrow\alpha$, respectively.

4) One spheroidal primary particle in the semisolid microstructure usually originates one equiaxed dendrite in the as-cast microstructure.

5) The variation of primary particle size with holding time does not obey the LSW law, $D_t^3 - D_0^3 = Kt$, after the semisolid system is up to solid-liquid equilibrium state due to the contribution of mergence.

6) Longer heating duration is beneficial for obtaining globular primary particles, but simultaneously it also leads their size to become larger.

References

[1] LIU D, ATKINSON H V, KAPRANOS P, JIRATTITICHAROEAN W, JONES H. Microstructural evolution and tensile mechanical properties of thixoformed high performance aluminium alloys [J]. Mater Sci Eng A, 2003, 361: 213−224.

[2] ATKINSON H V. Modeling the semisolid processing of metallic alloys [J]. Prog Mater Sci, 2005, 50: 341−412.

[3] FAN Z. Semisolid metal processing [J]. Int Mater Rev, 2002, 47: 49−85.

[4] FLEMINGS M C. Behavior of metal alloys in the semi-solid state [J]. Metall Trans A, 1991, 22: 957−981.

[5] StJOHN D H, QIAN M, EASTON M A, CAO P, HILDEBRAND Z. Grain refinement of magnesium alloys [J]. Metall Mater Trans A, 2005, 36: 1669−1679.

[6] NAMI B, SHABESTARI S G, MIRESMAEILI S M, RAZAVI H, MIRDAMADI S. The effect of rare earth elements on the kinetics of the isothermal coarsening of the globular solid phase in semisolid AZ91 alloy produced via SIMA process [J]. J Alloys Compd, 2010, 489: 570−575.

[7] ZHANG Q Q, CAO Z Y, LIU Y B, ZHANG Y F, ZHANG L, ZHANG M L, WU R Z. Effect of asymmetrical deformation on the microstructure evolution of semisolid AZ91D alloy [J]. Mater Sci Eng A, 2008, 488: 260−265.

[8] JI Z S, HU M L, SUGIYAMA S, YANAGIMOTO J. Formation process of AZ31B semi-solid microstructures through strain-induced melt activation method [J]. Mater Charact, 2008, 59: 905−911.

[9] YANG M B, SHEN J, PAN F S. Effect of TiC addition on semisolid isothermal heat treated microstructure of ZA84 magnesium alloy [J]. Mater Sci Technol, 2009, 25: 393−399.

[10] ZHAO Z D, CHEN Q, KANG F, SHU DY. Microstructural evolution and tensile mechanical properties of thixoformed AZ91D magnesium alloy with the addition of yttrium [J]. J Alloys Compd, 2009, 482: 455−467.

[11] ZHA M, WANG H Y, XUE P F, LI L L, LIU B, JIANG Q C. Microstructural evolution of Mg-5Si-1Al alloy during partial remelting [J]. J Alloys Compd, 2009, 472: L18−L22.

[12] CHEN T J, HAO Y, LI Y D, MA Y. Effect of solid solution treatment on semisolid microstructure of dendritic zinc alloy ZA27 [J]. Mater Sci Technol, 2008, 24: 1313−1320.

[13] GUNTHER R, HARTIG C, BORMANN R. Grain refinement of AZ31 by $(SiC)_P$: Theoretical calculation and experiment [J]. Acta Mater, 2006, 54: 5591−5597.

[14] QIAN M, CAO P. Discussions on grain refinement of magnesium alloys by carbon inoculation [J]. Scripta Mater, 2005, 52: 7415−7419.

[15] CHEN Qiang. Research on effect of AZ91D-Y billets prepared by different methods on semisolid forging [D]. Harbin: Harbin Institute of Technology, 2009: 83. (in Chinese)

[16] CHEN P C, ZHU L M, LI Z. Fundamental of Metal Forming [M]. Beijing: China Machine Press, 2003: 77. (in Chinese)

[17] LOUE W R, SUERY M. Microstructural evolution during partial remelting of AlSi7Mg alloys [J]. Mater Sci Eng A, 1995, 203: 1−13.

[18] WANG J L, SU Y H, TSAO C Y A. Structural evolution of conventional cast dendritic and spray-cast nondendritic structures during isothermal holding in the semisolid sate [J]. Scripta Mater, 1997, 12: 2003−2007.

[19] TZIMAS E, ZAVALIANGOS A. Evolution of near-equiaxed microstructure in the semisolid state [J]. Mater Sci Eng A, 2000, 289: 228−240.

(Edited by YANG Bing)